Journal of Asian Concrete Federation
Vol. 10, No. 1, pp. 7-13, June 2024
ISSN 2465-7964/ eISSN 2465-7972
DOI http://dx.doi.org/10.18702/acf.2023.10.1.7

ACF 10th CONFERENCE The 10th Conference of the Asian Concrete Federation

Technical Paper

Proportioning Study for Low-carbon Sulfate-resistant Concrete by Microbial Corrosion Testing

Tao Wang[*], Osamu Taniguchi, Taichi Shibano, Toshio Araki and Benjamin Koh Yong Jun

(Received: March 18, 2024; Revised: March 18, 2024; Accepted: June 19, 2024; Published online: June 24, 2024)

Abstract: In addition to water absorption and chloride permeability measurement, sulfate resistance testing by microbial corrosion was conducted on low-W/B concretes made using large amounts of supplementary cementitious materials, including GGBF slag, for use as sewage pipes. The corrosion testing was conducted in a corrosion chamber at 30°C with a H_2S concentration of 100 ppm, in which specimens were exposed to the environment under two conditions: one group in the gas and the other partially submerged in circulating sewage water. After exposure for one year, the corrosion rate in the partially submerged phase tended to be 1.3 to 2.9 times higher than in the gas phase. Also, the amount of corrosion was compared, with the corrosion products being examined by EPMA. Exposure to the gas phase and partially submerged phase was thus found to represent the stage of forming monosulfates and dihydrate gypsum and ettringite, respectively. Deterioration was found to proceed at a higher rate as the pH value on the concrete surfaces decreased. Within the range of this study, the addition of silica fume and small-size GGBF slag led to no appreciable effect.

Keywords: Microbial corrosion, Binder, Corrosion rate, EPMA, Deterioration process.

1. Introduction

Concrete used for sewage tunnels is exposed to sulfates produced by microbes from hydrogen sulfide (H_2S) generated from sewage. This is known to cause expansion of concrete surfaces due to decomposition of cement hydrates and formation of gypsum and ettringite, progressively leading to surface erosion. Test methods for sulfate resistance include sulfuric acid immersion testing to investigate various properties to resist the acid using a 5% solution of sulfuric acid. Another approach to evaluation is microbial corrosion testing simulating actual environments of concrete. This is a method whereby concrete specimens are exposed to sewage water taken from a sewer pipe in service and a H_2S environment to induce microbial sulfate deterioration. As the evaluation standard, we refer to the japanese manual on corrosion inhibition and prevention technologies for sewerage concrete structures. This kind of testing has conventionally been conducted using concrete with relatively low strength with a W/B of 50% or more [1]. Here, we concentrate to a lower W/B of 40% or less to test.

Accordingly, the authors conducted microbial corrosion tests using concretes with a W/B of 40% or less, while substantially reducing the cement content to make the concrete a low-CO2 type and varying the contents of supplementary cementitious materials(binder) over a period of 1 year in an

---

[*] **Corresponding author Tao Wang** *Wang is a Section Chief at Institute of Technical Research, Penta-Ocean Construction Co., Ltd., Tochigi, Japan. Email: tao.wang@mail.penta-ocean.co.jp*
Osamu Taniguchi *is Group Leader at Institute of Technical Research, Penta-Ocean Construction Co., Ltd., Tochigi, Japan. Email: osamu.taniguchi@mail.penta-ocean.co.jp*
Taichi Shibano *is Group Leader at Institute of Technical Research, Penta-Ocean Construction Co., Ltd., Tochigi, Japan. Email: osamu.taniguchi@mail.penta-ocean.co.jp*
Toshio Araki *is Director General at International Civil Engineering Divisions Gr, Penta-Ocean Construction Co., Ltd., Singapore. Email: toshio.araki@mail.penta-ocean.co.jp*
Benjamin Koh Yong Jun *is Manager at Koh Brothers Building & Civil Engineering Contractor Pte. Limited., Singapore. Email: benjaminkoh@kohbrothers.com*
From Special Issue - 10th Asian Concrete Federation Conference

Table 1 – List of materials.

Item	Material name	Abbreviation	Physical properties
Binder	Cement	OPC	D=3150 B=3320
	Blast furnace fine powder 4	GGBFS	D=2890 B=4440
	Silica fume	SF	D=2200 B=180000
	Blast furnace fine powder 8	BFF P8000	D=2920 B=8180
	Limestone fine powder	UFLSP	D=2700 B=3850
Fine aggregate	River sand	Natural Sand	D=2620 War=0.7
	Crushed sand	Rock Sand	D=2620 War=0.62
	Blast furnace slag	Slag Sand	D=2650 War=1.03
Coarse aggregate	Crushed stone	20∼10mm	D=2620 War=0.44
	Gravel	10∼5mm	D=2620 War=1.2
Admixture	High performance water reducing agent	Ad1	Polycarboxylic acid ether polymer
	AE water reducing agent	Ad2	Polycarboxylic acid compound
	Pore blocker admixture	Ad3	Hydrophobic pore blocking component

Note: 1) D = density ($\mathrm{kg/m^3}$), the density of aggregate is the surface dry density.
2) B = Brain specific surface area ($\mathrm{cm^2/g}$), War = Water absorption rate (%).

environment with a H_2S concentration of 100 ppm. Specimens were set in the gas phase and the intermediate phase of sewage and gas to measure the corrosion depth and calculate the corrosion rate. After testing, specimens were subjected to electron probe microanalysis (EPMA) to identify the corrosion products to evaluate the vulnerability to deterioration process. Note that these tests were based on BS and ASTM as part of the investigation prior to the second phase of the DTSS construction in Singapore.

2. Experimental Plan

2.1. Materials and mixture proportions

Table 1 lists the materials and ordinary Portland cement, ground granulated blast furnace slag with a blain fineness of 4,000 and 8,000 $\mathrm{cm^2/g}$, and limestone powder were used as binders. Fine aggregates were river sand, crushed sand, and slag sand. Here, unit aggregate amount is 800 $\mathrm{kg/m^3}$ for all of mixture. A hydrophobic pore blocker, which reduces the water absorption and water permeability of concrete, was also used as a chemical admixture.

Concrete was proportioned with a binder containing more than 80% blast furnace slag with or without silica fume with varying percentages of other supplementary cementitious materials to consume calcium hydroxide in the binder (Table 2). The water-binder ratio was set at 30 to 35% to achieve a target strength of more than 60 MPa. Mixtures A and G made using slag sand (A-SS and G-SS) were also tested in expectation of forming chip-resistant dihydrate gypsum coating [2]. Specimens made using only cement with no other binder (OPC) were also fabricated to compare the sulfate resistance.

2.2. Test methods

(1) Concrete properties

Table 3 gives the test items for hardened concrete. These are conducted to compare various properties and sulfate resistance of the concretes.

(2) Microbial corrosion test

(a) Test apparatuses and exposure conditions

The microbial corrosion test apparatus consists of a H_2S gas supply system, sewage circulation system, coolant system, control system, and corrosion chamber, which is adjusted to maintain an environment temperature of 30 °C, relative humidity of 100%, and H_2S gas concentration of 100 ppm.

The corrosion chamber contains a four-layer tray structure, with each tray holding wastewater to a depth of 4 cm to allow testing of four specimens in the upper gas phase, or in the lower partially submerged phase. Sewage water taken directly from a sewage pump station is held in the trays and replaced with newly taken sewage water every two weeks.

The bottom surfaces of gas-phase specimens, which

Table 2 – Unit amount of concrete mixtures.

S/N	Mixes	Water-binder ratio	W/B	Binder					Admixtures			Fine aggregates			Fine aggregate size	
				OPC	GGBS	SF	BFF P8000	UFLSP	ad1	ad2	ad3	Natural Sand	Crushed Rock	BF-Slag Sand	20mm	10mm
S No.	Mix ID	kg/m^3	%	kg/m^3	kg/m^3	kg/m^3	kg/m^3	kg/m^3	Ml/100 kg binder		L/m^3	kg/m^3	kg/m^3	kg/m^3	kg/m^3	kg/m^3
0	OPC	175	35	500	-	-	-	-	-	-	-	400	400	-	575	285
1	A	150	30	100	400	-	-	-	600	500	2	400	400	-	575	285
2	B	150	30	50	450	-	-	-	600	500	2	400	400	-	575	285
3	C	160	31	50	450	10	-	-	800	350	2	400	400	-	575	285
4	D	170	34	50	350	75	25	-	1000	400	2	400	400	-	575	285
5	E	170	34	50	375	75	-	-	1000	450	2	400	400	-	575	285
6	F	160	32	5	400	25	25	-	1550	-	2	400	400	-	575	285
7	G	160	32	50	425	25	-	-	1500	-	2	400	400	-	575	285
8	H	160	3	50	375	-	25	50	1500	-	2	400	400	-	575	285
9	A-SS	170	34	100	400	-	-	-	500	50	2	-	-	800	575	285
10	G-SS	170	34	50	425	25	-	-	600	50	2	-	-	800	575	285

Table 3 – List of test items.

Test Items	Standard	Age (days)
Compressive strength	BS EN12390-3:2019	28
Volume of permeable voids	ASTM C642	28
Chloride permeability test	ASTM C1202	28

are set at a height of 170 mm from the bottom of the sewage water, are exposed to H_2S gas in the chamber, so as to be prone to the effect of sulfate corrosion to simulate the environments of concrete tunnel ceilings of sewage pipes. Partially submerged specimens simulate corrosion environments of partially submerged concrete by immersing each specimen in sewage water to a depth of 20 mm.

Twelve specimens were tested for each mixture type, with six specimens each being placed in the gas and partially submerged phases. Each specimen measuring 10 by 7 by 5 cm is encased in a steel frame (Photo 1), with a resin being injected in the space between the frame and specimen to protect all five surfaces other than the exposure surface (10 by 7 cm) from being exposed.

(b) Measurement items of sulfate resistance

- Weight loss

The weight of each specimen is measured at the beginning and end of exposure. The weight loss divided by the exposure surface area and the exposure time is calculated as the weight loss during the exposure time $(\mathrm{kg/m^2/year})$.

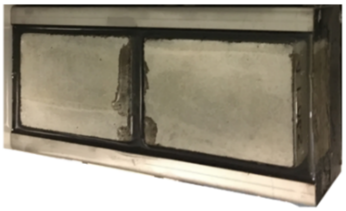

Fig. 1 – A test piece in a steel frame before exposing

- Corrosion rate

The corrosion rate is measured by photogrammetry. After washing corroded specimens, five photographs are taken per specimen. A 3D image of the exposure surface is then produced to calculate the mean surface height with respect to the datum surface of the steel frame. The difference between the mean surface heights before and after exposure is taken as the thickness of corrosion, with the corrosion rate, γ(mm/year), being determined by dividing the corrosion thickness, $\mathrm{D_t}$ (mm), by the corrosion time, $\mathrm{t_i}$ (year).

- EPMA of element distribution

The distribution of elements on specimens after microbial corrosion testing is measured by JSCE-G574-2013 (area analysis method of elements distribution in concrete by using EPMA). Electron probe microanalysis is conducted on mixtures A, E, A-SS, and OPC. Representing the analysis surface, the sample size is 5 by 5 by 2 cm, which is cut from central section of specimen.

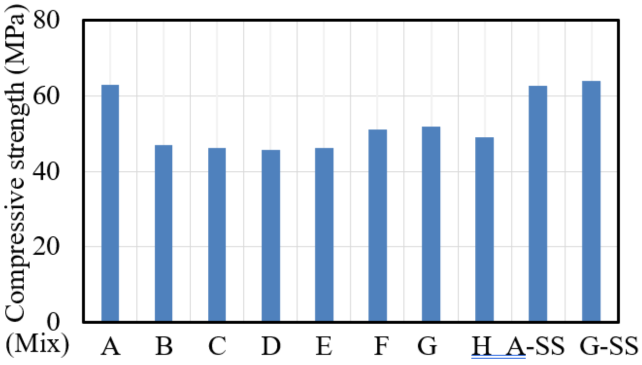

Fig. 2 – Compression tests

3. Results and discussion

3.1. Concrete properties

Fig. 2 shows the results of compression tests at 28 days. Here, all specimens were cured in water without corrosion, and their compressive strengths were measured. The strength of mixture A, A-SS and G-SS showed high strength passing 60 $\mathrm{N/mm^2}$. From the result, the strength of concrete has been increased by the use of mixed slag sand.

Fig. 3 shows the volume ratio of permeable voids and chloride permeability. No correlation is found between these items, with mixture A showing a high chloride permeability despite the low void ratio.

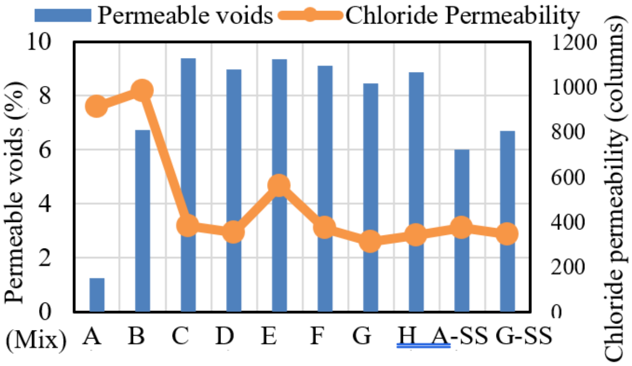

Fig. 3 – Volume ratio of permeable voids and chloride permeability

Due to the mixture A with a low void ratio, compressive strength of mixture A was higher than others, being consistent with the study by Sugi, et al. [3]. On the other hand, the void ratio of mixture A-SS containing slag sand was 6.03 %, being five times as high as that of mixture A (1.27%). From this result, the denseness of mixture A-SS should be poorer than that of mixture A. Compressive strength of mixture A-SS should become lower than mixture A. Actually, both of mixture A and A-SS have a similar strength level. It is assumed that there is a resilient interfacial transition zone between aggregate and paste about mixture A-SS.

Table 4 – Comparison of appearance of specimen surfaces before washing

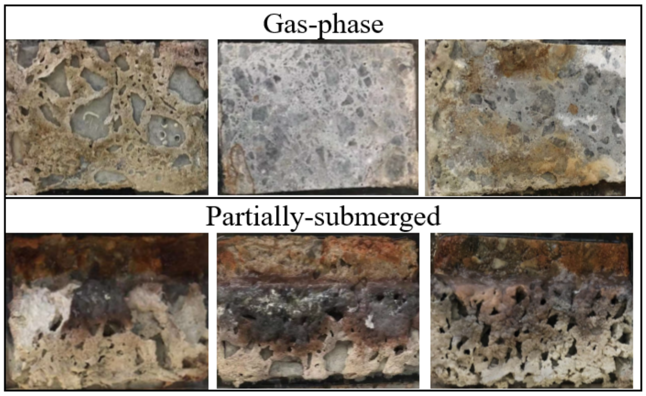

The chloride permeability of mixture G is the lowest among the mixtures. By comparing mixtures A and B with mixtures C through G containing silica fume (300 to 600 columns), the use of silica fume is found to reduce the chloride permeability, in agreement with the study by Mashimo, et al. [4].

3.2. Sulfate resistance

(1) Surface conditions by corrosion

Table 4 shows the appearance of specimen surfaces before washing at the end of microbial corrosion testing for one year. More smudge and corrosion substances accumulate on partially submerged specimens than on those in the gas phase. Also, among the gas-phase specimens of mixtures OPC, A-SS, and A, the adhesion of smudge and corrosion substances is minimal on mixture A, followed by A-SS and OPC in this order, suggesting that concrete surfaces with certain properties are less prone to aerobe propagation. Table 5 shows a comparison of typical surfaces of specimens after washing (gas-phase specimens of OPC and A). The surface of OPC represents significant erosion, showing surface paste elution and aggregate exposure due to microbial corrosion. On the other hand, the specimen of mixture A shows high resistance to sulfate with little erosion.

Table 5 – Comparison of typical surfaces of specimens after washing

Gas-phase specimens of OPC	
Full surface	Local enlargementg
	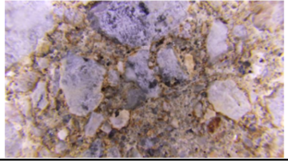
Gas-phase specimens of A	
Full surface	Local enlargement
	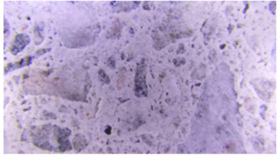

(2) Weight loss

Fig. 4 shows the weight losses of specimens after an exposure period of 1 year. The losses of partially submerged specimens tend to be greater than gas-phase specimens, due to the above-mentioned high surface acidity. It is also found that partially submerged specimens of mixture OPC underwent large losses, presumably because a large amount of $Ca(OH)_2$ was consumed, causing progressive precipitation of dihydrate gypsum and ettringite followed by subsequent dissolution.

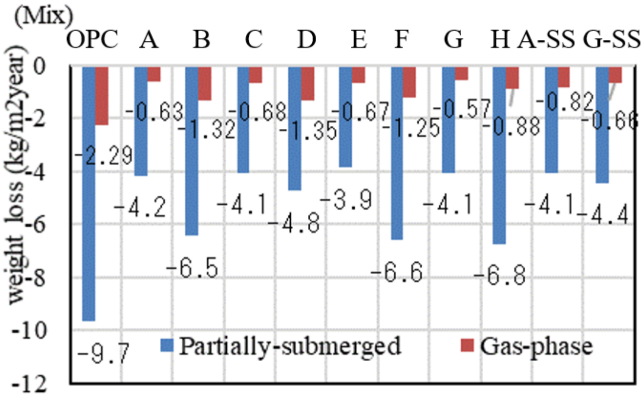

Fig. 4 – The weight losses

(3) Corrosion rate

Fig. 5 shows the corrosion rate after exposure for one year. The corrosion rate of gas-phase specimens excepting mixture OPC ranges from 2.0 to 5.0 mm/year, whereas that of partially submerged specimens ranges from 4.0 to 11.0 mm/year, being twice as high as the rate of gas-phase specimens. In addition, the corrosion rate is measured by photogrammetry. After washing corroded specimens, five photographs are taken per specimen. A 3D image of the exposure surface is then produced to calculate the mean surface height with respect to the datum surface of the steel frame.

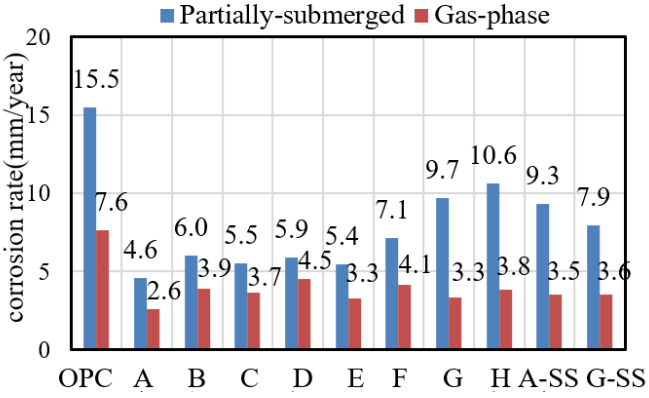

Fig. 5 – The corrosion rate

The corrosion rate of both gas-phase and partially submerged specimens of mixture A is the lowest. Concrete containing a large proportion of GGBF slag in place of cement is known to improve sulfate resistance in the literature [5]. Within the range of this study, however, the results of mixture A with a GGBF slag replacement ratio of 80% predominate over mixture B with a replacement ratio of 90%. Also, the corrosion rate of mixture D containing BFF P8000 shows no significant difference from mixture E made using GGBF slag with no BFF P8000. The corrosion rate of mixture C containing silica fume is on a level similar to mixture B containing no silica fume, suggesting that silica fume is not presumed to contribute to the improvement of sulfate resistance.

Also, the corrosion rate of mixture A-SS made using slag sand tends to be higher than mixture A with no slag sand. As a method of evaluating sulfate resistant concrete, immersion in an aqueous solution of sulfuric acid generally leads to high resistance of concrete containing silica fume, GGBF slag, and slag sand, but the results of the present microbial corrosion tests did not agree with this. It is therefore considered that these differences are caused by different corrosion methods in this study.

Table 6 – EPMA results of specimens subjected to microbial corrosion

Item	Gypsum dihydrate	Ettringite	Monosulfates	Calcium hydroxide	C-S-H gel
Chemical formula of the component	$CaSO_4 .2\,H_2O$	$3\,CaO \cdot Al_2O_3$ $3\,CaSO_4 \cdot 2\,H_2O$	$3\,CaO \cdot Al_2O_3 \cdot$ $CaSO_4 \cdot 12\,H_2O$	$Ca(OH)_2$	$3\,CaO \cdot SiO_2$ $\cdot 3\,H_2O$
S/Ca molar ratio	1/1=1	3/6=0.5	1/4=0.25	0/1=0	0/1=0
Molar ratio ranges	S/Ca =1.0 0.5		S/Ca =0.25 0		

Mixture-A(Partially-submerged)
↓surface deterioration

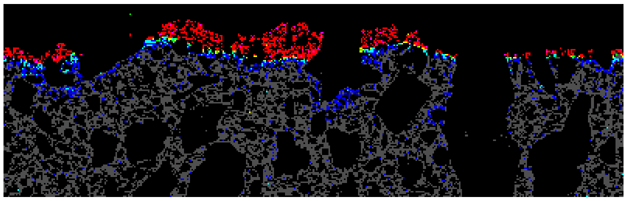

Mixture-E (Partially-submerged)
↓surface deterioration

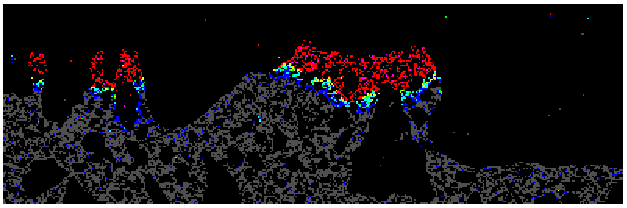

ranges of S/Ca molar ratio:0.6 1.0 (red)

Mixture-OPC (Gas-phase)
↓surface deterioration

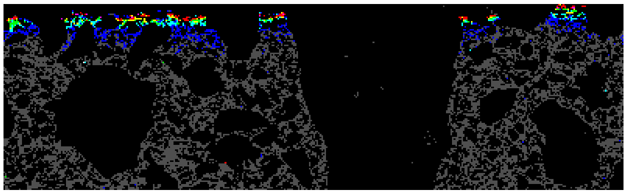

Mixture-A (Gas-phase)
↓surface deterioration

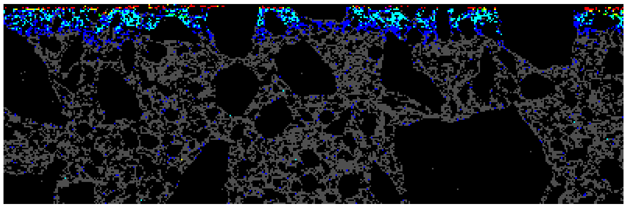

ranges of S/Ca molar ratio: 0.05 0.20 (blue indigo)

(5) EPMA

Table 6 shows typical EPMA results of specimens subjected to microbial corrosion. The S/Ca molar ratio in the deteriorated layers of partially submerged specimens, in which the surface pH value of concrete is low, of mixtures A and E ranges from 0.6 to 1.0, suggesting that the main components are dihydrate gypsum and ettringite. The depth of the deteriorated layer ranges from 4.0 to 6.3 mm.

On the other hand, the S/Ca molar ratio in the deteriorated layers of gas-phase specimens, in which the surface pH value of concrete is relatively high, of mixtures OPC and A ranges from 0.05 to 0.2, suggesting that that the deterioration products in the surface layer are primarily components close to monosulfates. Based on these results, the condition of concrete in the gas phase after exposure to the microbial corrosion environment is presumed to be a condition of a stage prior to the formation of dihydrate gypsum and ettringite. The depth of the surface deterioration layer was around 2.8 mm. These results also reveal that the specimen surfaces tend to be more prone to deterioration as the pH values decrease. These results indicate a viable possibility of evaluating surface layer deterioration by dividing the deterioration process into three stages according to the corrosion environment: Stage I where the pH value of specimens decreases, leading to formation of hydrogen sulfide due to microbial activities; Stage II where ettringite is formed, causing cracks due to surface expansion; and Stage III where surface ettringite turns into dihydrate gypsum, embrittling the surface layer.

4. Conclusion

1. No decrease in volume ratio of permeable void was observed due to the inclusion of slag aggregate. Also, the incorporation of silica fume tended to reduce the chloride permeability.

2. Within the range of this study, the mixture with a binder consisting of 20% cement and 80% GGBF slag led to the lowest rate of sulfate corrosion. The mixture made using GGBF slag with a specific surface of 8,000 cm^2/g and slag sand led to no

enhancement in the sulfate resistance.

3. The corrosion rate in the partially submerged phase tended to be 1.3 to 2.9 times higher than in the gas phase.

4. Deterioration products were identified by S/Ca mapping through EPMA. Exposure to the gas phase and partially submerged phase was thus found to represent the stage of forming monosulfates and the stage of forming dihydrate gypsum and ettringite, respectively.

By adding large amounts of industrial waste to concrete, it can be used in highly corrosive sewage environments. In the future, we will reconsider the composition of the mix by measuring concrete deterioration in an actual environment.

Acknowledgement

This study was carried out jointly by Penta Ocean Construction Co., Ltd. and Koh Brothers Building and Civil Engineering Contractor Pte. Limited, and was applied to the concrete lining of The Deep Tunnel Sewerage System Phase 2 in Singapore.

References

[1] Sasaki, A., Takahashi, T., Shindo, T., & Toyama, K. (2008). Durability of sulfuric acid resistant concrete in sewage environment. *Proceedings of the Japan Concrete Institute*, *30*(1), 633–638.

[2] Paweena, J., Hosoya, T., Fujii, T., & Ayano, K. (2013). Study on improvement of sulfuric acid resistance of concrete by bf slag fine aggregate. *Journal of JSCE*, *69*(4), 337–347.

[3] Sugi, D., Tsukagoshi, M., & Ueda, T. (2013). Long-term durability and microstructure of precast concrete members using fly ash and blast furnace slag fine powder. *Proceedings of the Japan Concrete Institute*, *35*(1), 763–768.

[4] Mashimo, M., Fukute, T., Hamada, H., & Watanabe, K. (1995). Evaluation by rapid chlorine permeability test of high-strength concrete with various admixtures added. *Proceedings of the Japan Concrete Institute*, *17*(1), 979–984.

[5] Hatanaka, N., Kurashige, I., & Uomoto, K. (2002). Improving the sulfuric acid resistance of concrete with various admixtures. *Japan Society of Civil Engineers 2002 Annual Meeting*, *539*, 1077–1078.